SETAC PRESS

Environmental Toxicology and Chemistry, Vol. 33, No. 10, pp. 2197–2207, 2014

Printed in the USA

Surface Complexation Modeling

MODELING SELENIUM (IV AND VI) ADSORPTION ENVELOPES IN SELECTED TROPICAL SOILS USING THE CONSTANT CAPACITANCE MODEL

MARIANA BASSETTO GABOS,†‡ SABINE GOLDBERG,‡ and LUÍS REYNALDO FERRACCIÚ ALLEONI*†
†University of São Paulo, Piracicaba, São Paulo, Brazil
‡Salinity Laboratory, US Department of Agriculture, Riverside, California, USA

(Submitted 29 October 2013; Returned for Revision 16 December 2013; Accepted 7 March 2014)

Abstract: The adsorption of selenium (Se) on soil is important because of the relevance of Se to environmental and health issues. The adsorption of Se(IV) and Se(VI) was evaluated on soil samples from São Paulo State, Brazil, as a function of varying pH, and the experimental data were fitted to the constant capacitance model. Adsorption experiments were conducted for 15 soil samples, after the addition of 20 μmol L^{-1} of either Se(IV) or Se(VI), and the adjusted pH ranged between 2.5 and 10. Selenite adsorption was high for all soils, decreased with increasing pH, and was strongly correlated with Fe and Al oxide content. In contrast, Se(VI) adsorption was very low at pH values commonly found in agricultural soils, except for the highly weathered Rhodic Acrudox. The constant capacitance model fitted the Se(IV) and Se(VI) adsorption data well. Optimizations of mono- and bidentate complexation and surface protonation constants were used for the Se(IV) adsorption data. For Se(VI), optimizations for the 2 monodentate species were employed. *Environ Toxicol Chem* 2014;33:2197–2207. © 2014 SETAC

Keywords: Selenite Selenate Soil pH Brazilian soils FITEQL

INTRODUCTION

Selenium (Se) is a metalloid present in trace amounts in all biogeochemical environments. Low quantities of Se are essential for animal and human nutrition. The recommended daily intake for an adult is 40 μg to 55 μg [1], although Se can have deleterious effects on health in a narrow concentration range (40–400 μg/d). The presence of Se in food is strongly correlated to the concentration of Se in the soils where the food was grown [2]. Selenium has not been proven to be a required micronutrient for plants, but it can accumulate in plant tissues and can produce toxic symptoms in extreme cases [3]. Accumulation of Se in plants is important because ingestion of plants is the main pathway by which Se enters the food chain. Both Se toxicity and Se deficiency are the result of Se content in soils and Se behavior in different soil phases.

The amount of Se in soils depends on natural sources or human activities. Both Se-deficient and Se-contaminated areas have been reported [4]. Deficient areas require strategies for crop and livestock amendment. Soil fertilization is an option that has been adopted in some areas, such as Finland [5]. The behavior of Se in soils is mostly pH dependent. Thus, a knowledge of the effect of pH on Se adsorption is important mainly in highly weathered humid tropical soils, for which studies are scarce.

Two forms of Se usually found under natural soil conditions are selenite (SeO_3^{2-}; Se[IV]) and selenate (SeO_4^{2-}; Se[VI]), which behave differently in soils. Selenite forms strong bonds with soil surfaces as inner-sphere complexes [6], and for this reason is considered less available from an environmental perspective. Selenate is less adsorbed in soil and consequently more bioavailable [7] because it forms outer- and inner-sphere complexes, as several authors have reported for pure minerals [8–11].

Selenium adsorption occurs on soil sites with net positive balance of charges particularly present on the surface of sesquioxides. Selenium adsorption in pure minerals has been studied to better understand the relationship between Se(IV) and Se(VI) and soil colloids, yielding some interesting results. For example, Se adsorption was positively correlated with free Fe oxide content [12,13], and pH was negatively correlated with Se(IV) and Se(VI) adsorption [7,14].

Surface complexation models based on a thermodynamic approach are able to describe surface species, mass balance, and chemical reactions [15]. Empirical models, such as Freundlich and Langmuir, are valid only for the conditions under which the experiment was conducted [16]. The constant capacitance model has been used successfully to describe Se adsorption in soils [16–18]. The constant capacitance model includes 4 assumptions. First, only inner-sphere complexes are formed. Second, anion adsorption occurs via a ligand exchange mechanism with reactive surface hydroxyl groups. Third, ions from the background electrolyte do not form surface complexes. Fourth, the relationship between surface charge and surface potential is linear [15].

In the present study, we investigated the sorption of Se(IV) and Se(VI) on 15 tropical soils from São Paulo State in Brazil. The constant capacitance model was fit to the experimental data as a function of varying pH in the equilibrium solution.

MATERIALS AND METHODS

Fifteen soils with contrasting attributes (texture, Al and Fe oxides, and organic carbon content) were selected from soil orders representative of the Brazilian state of São Paulo (Table 1). All soil samples were collected from the upper layer (0.0–0.2 m) in areas with native vegetation. A subsurface sample (1.2–1.6 m) of the Rhodic Acrudox (LVwf-B) was also collected because of its net positive balance of charge, thus representing conditions of extreme weathering as a result of a low presence of organic matter. Samples were air dried, crushed, and passed through a 2-mm sieve.

* Address correspondence to alleoni@usp.br
Published online 12 March 2014 in Wiley Online Library (wileyonlinelibrary.com).
DOI: 10.1002/etc.2574

Table 1. Classification and chemical characteristics of soils

Soil	pH_{water}[a]	Clay ($g\,kg^{-1}$)	OC ($g\,kg^{-1}$)	IOC ($\mu g\,g^{-1}$)	SA ($m^2\,g^{-1}$)	Fe ($g\,kg^{-1}$)	Al ($g\,kg^{-1}$)	CEC ($mmol_c\,kg^{-1}$)	*S*OH ($mmol\,kg^{-1}$)
CX (sandy-clay-loam, Typic Haplustept)	4.3	243	14.4	—[b]	38.9	19.3	2.3	22.7	5.96
GM (clay, Aquic Haplohumults)	4.9	476	118.5	—[b]	105.3	4.9	4.8	50.4	16.16
LA-1 (sandy-clay-loam, Xanthic Hapludox)	4.8	222	18.9	—[b]	25.9	19.7	2.2	23.4	3.97
LAwf (clay, Anionic Acrudox)	4.7	470	26.1	—[b]	88.4	113.3	3.9	16.9	13.57
LV-2 (clay, Rhodic Eutrudox)	4.6	530	29.9	—[b]	60.4	86.6	5.1	30.6	9.26
LVA-2 (sandy-clay-loam, Typic Hapludox)	4.2	221	14.4	—[b]	6.2	13.6	1.2	15.5	0.94
LVef (clay, Rhodic Hapludox)	7.3	684	51.1	178.6	86.5	185.2	4.4	60.4	13.26
LVwf- A horiz. (clay, Rhodic Acrudox)	4.7	716	15.3	—[b]	92.4	208.2	5.7	23.7	14.19
LVwf- B horiz. (clay, Rhodic Acrudox)	5.6	663	8.7	—[b]	56.2	232.0	6.1	23.7	8.63
MT (clay, Mollic Hapludalfs)	5.8	543	29.8	—[b]	165.6	113.3	4.7	105.5	25.40
NVef (clay, Rhodic Eutrudult)	5.5	658	29.7	—[b]	90.3	192.2	4.8	61.1	13.86
PV-2 (sandy loam, Typic Rhodudalfs)	5.7	427	22.2	—[b]	64.8	51.3	2.0	54.4	9.94
PVA-3 (loam, Typic Hapludults)	5.4	247	18.7	—[b]	25.7	32.9	4.4	44.6	3.94
RL (loam, Lithic Dystrudepts)	5.9	142	14.3	—[b]	34.3	7.5	0.3	33	5.27
RQ (loamy sand, Typic Quartzipsamment)	4.4	80	4.3	—[b]	2.0	3.0	0.6	7.6	0.30

[a]pH in water extract.
[b]Below detection limit ($150\,\mu g\,g^{-1}$).
OC = organic carbon; IOC = inorganic carbon; SA = specific surface area (Cihacek and Bremner [19]); Fe and Al = dithionite-citrate-bicarbonate (Coffin [20]); *S*OH = total number of reactive sites.

Some soil chemical characteristics are given in Table 1. The pH was measured potentiometrically in a 1:2.5 soil:water solution. Carbon components were determined by a carbon coulometer. Total carbon was determined by furnace combustion at 950 °C; inorganic carbon was measured using the acidification module and heating; and organic carbon content was calculated as the difference between total and inorganic carbon. Specific surface area was determined by Cihacek and Bremner's [19] method, using ethylene glycol monoethyl ether adsorption. Free Fe and Al were extracted by sodium dithionite-citrate-bicarbonate (DCB) [20], and the contents were determined via inductively coupled plasma (ICP) emission spectrometry. The cation exchange capacity was determined by the compulsive exchange method proposed by Gillman [21] for highly weathered soils. Data on mineralogy and additional information about our soil samples can be found in Soares [22].

The adsorption envelope experiment was carried out in a batch system. One gram of soil and 25 mL of solution were added to 50-mL polypropylene centrifuge tubes. For both Se(IV) and Se(VI), the concentration was $20\,\mu mol\,L^{-1}$, added as Na_2SeO_3 and Na_2SeO_4, respectively. The pH varied from 2.5 to 10 and was adjusted by adding either $1.0\,mol\,L^{-1}$ HCl or $1.0\,mol\,L^{-1}$ NaOH solutions. The supporting electrolyte was $0.1\,mol\,L^{-1}$ NaCl, and the reaction time was 2 h on a reciprocating shaker at room temperature (24.5 ± 0.2 °C). Solutions were subsequently centrifuged for 20 min at 10 062 *g* force, the pH of the supernatant solutions was determined, and the solution was passed through a 0.45-μm membrane filter. The Se concentration was determined in all solutions by using ICP emission spectrometry. The concentration of adsorbed Se was calculated as the difference between the amount added and the amount remaining in solution after equilibrium. As observed by Goldberg et al. [16] and Hyun et al. [13], the oxidation of Se(IV) to Se(VI) during the adsorption process was lower than 10%, even with shaking times longer than 2 h. For this reason, Se oxidation was not taken into account in the present study.

The constant capacitance model [23] was fit to the Se(IV) and Se (VI) adsorption data, as described in detail by Goldberg et al. [24]. Previous investigations have been successful in applying the constant capacitance model to soils [16–18]. For this reason, the model was chosen over the 2-layer surface complexation model, which also defines inner-sphere surface complexes [25]. The FITEQL 4.0 computer software [26] fits the surface complexation constants to the sorption data using a nonlinear least squares optimization routine [27]. The acid dissociation constants (pK_a) for selenic acid ($pK_{a1} = 2.46$, $pK_{a2} = 9.77$) and selenious acid ($pK_{a2} = 1.92$) were included in the model optimizations. Considering *S*OH as a functional group of oxide minerals from the clay particle soil fraction, protonation and deprotonation are defined as

$$SOH_{(s)} + H^+_{(aq)} \leftrightarrow SOH^+_{2(s)} \quad (1)$$

$$SOH_{(s)} \leftrightarrow SO^-_{(s)} + H^+_{(aq)} \quad (2)$$

The surface complexation reactions with Se(IV) are presented in Equations 3, 4, and 5, and the reactions with Se(VI) are described in Equations 6, 7, and 8

$$SOH_{(s)} + H_2SeO_{3(aq)} \leftrightarrow SHSeO_{3(s)} + H_2O \quad (3)$$

$$SOH_{(s)} + H_2SeO_{3(aq)} \leftrightarrow SSeO^-_{3(s)} + H^+_{(aq)} + H_2O \quad (4)$$

$$2SOH_{(s)} + H_2SeO_{3(aq)} \leftrightarrow S_2SeO_{3(s)} + 2H_2O \quad (5)$$

$$SOH_{(s)} + H_2SeO_{4(aq)} \leftrightarrow SHSeO_{4(s)} + H_2O \quad (6)$$

$$SOH_{(s)} + H_2SeO_{4(aq)} \leftrightarrow SSeO^-_{4(s)} + H^+_{(aq)} + H_2O \quad (7)$$

$$2SOH_{(s)} + H_2SeO_{4(aq)} \leftrightarrow S_2SeO_{4(s)} + 2H_2O \quad (8)$$

The intrinsic equilibrium constants considered for the previously described complexation reactions are

$$K_+(\text{int}) = \frac{[SOH_2^+]}{[SOH][H^+]}\exp(F\psi/RT) \quad (9)$$

$$K_-(\text{int}) = \frac{[SO^-][H^+]}{[SOH]}\exp(-F\psi/RT) \quad (10)$$

$$K^1_{Se(IV)}(\text{int}) = \frac{[SHSeO_3]}{[SOH][H_2SeO_3]} \quad (11)$$

$$K^2_{Se(IV)}(\text{int}) = \frac{[S\text{SeO}_3^-][\text{H}^+]}{[S\text{OH}][\text{H}_2\text{SeO}_3]}\exp(-F\psi/RT) \quad (12)$$

$$K^3_{Se(IV)}(\text{int}) = \frac{[S_2\text{SeO}_3]}{[S\text{OH}]^2[\text{H}_2\text{SeO}_3]} \quad (13)$$

$$K^1_{Se(VI)}(\text{int}) = \frac{[S\text{HSeO}_4]}{[S\text{OH}][\text{H}_2\text{SeO}_4]} \quad (14)$$

$$K^2_{Se(VI)}(\text{int}) = \frac{[S\text{SeO}_4^-][\text{H}^+]}{[S\text{OH}][\text{H}_2\text{SeO}_4]}\exp(-F\psi/RT) \quad (15)$$

$$K^3_{Se(VI)}(\text{int}) = \frac{[S_2\text{SeO}_4]}{[S\text{OH}]^2[\text{H}_2\text{SeO}_4]} \quad (16)$$

where F is the Faraday constant (C mol_c^{-1}), ψ is the surface potential (V), R is the universal gas constant ($\text{J mol}^{-1}\ \text{K}^{-1}$), T is absolute temperature (K), and species in brackets are their concentrations (mol L^{-1}). Bidentate bonds require at least twice as many sites as are required in the monodentate surface complexes [27]. For this reason, in the bidentate equations (Equations 13 and 16), the surface functional group terms were squared.

The mass balances of the surface functional groups for monodentate and bidentate, respectively, for Se(IV) are

$$[S\text{OH}]_T = [S\text{OH}] + [S\text{OH}_2^+] + [S\text{O}^-] + [S\text{HSeO}_3] + [S\text{SeO}_3^-] \quad (17)$$

$$[S\text{OH}]_T = [S\text{OH}] + [S\text{OH}_2^+] + [S\text{O}^-] + 2[S_2\text{SeO}_3] \quad (18)$$

The mass balances for Se(VI) (monodentate and bidentate) are

$$[S\text{OH}]_T = [S\text{OH}] + [S\text{OH}_2^+] + [S\text{O}^-] + [S\text{HSeO}_4] + [S\text{SeO}_4^-] \quad (19)$$

$$[S\text{OH}]_T = [S\text{OH}] + [S\text{OH}_2^+] + [S\text{O}^-] + 2[S_2\text{SeO}_4] \quad (20)$$

The expressions of charge balance for monodentate are

$$\text{Se(IV)} : \sigma = [S\text{OH}_2^+] - [S\text{O}^-] - [S\text{SeO}_3^-] \quad (21)$$

$$\text{Se(VI)} : \sigma = [S\text{OH}_2^+] - [S\text{O}^-] - [S\text{SeO}_4^-] \quad (22)$$

The charge balance expression for bidentate for both redox states is

$$\sigma = [S\text{OH}_2^+] - [S\text{O}^-] \quad (23)$$

where σ is the surface charge ($\text{mol}_c\ \text{L}^{-1}$). The surface potential is related to the surface charge according to Equation 24, in which C is capacitance (F m^{-2}), S_a is surface area ($\text{m}^2\ \text{g}^{-1}$), and C_p is suspension density (g L^{-1}).

$$\sigma = \frac{CS_aC_p}{F}\psi \quad (24)$$

The FITEQL initial inputs were taken from previous studies. The capacitance value that we used in the present study ($C = 1.06\ \text{F m}^{-2}$) was considered optimum for Al oxide by Westall and Hohl [28]. The protonation and the deprotonation constants were log $K_-(\text{int}) = -8.95$ and log $K_+(\text{int}) = 7.35$, following Goldberg and Sposito [29]. The number of the reactive sites was recommended by Davis and Kent [30] for natural materials as $N_s = 2.31$ sites nm^{-2}; this information is necessary to calculate the total sites, as shown by Karamalidis and Dzombak [25]. Variance or goodness-of-fit (V_y) was calculated by the software as

$$V_Y = \frac{SOS}{df} \quad (25)$$

where SOS is the weighted sum of squares of residuals and df is degrees of freedom [26]. Values of $V_Y < 20$ are considered a reasonably good fit [26].

RESULTS AND DISCUSSION

Effect of pH on Se(IV) adsorption

Selenite adsorption was high for the majority of the soils examined (Figures 1–3). The 3 exceptions (LVA-2, RL, and RQ; Figure 3) were sandy-textured soils, which have the lowest number of sites for adsorption. For all soils Se(IV) adsorption decreased with increasing pH of the solution. This behavior is a consequence of the decrease in the number of positive charges on the variable charge soil components. In humid tropical soils, positive charges are attributed to sesquioxides and organic matter [31]. Several researchers have reported decreasing Se(IV) adsorption as a function of increasing pH [14,18,32]. Soil acidity is commonly corrected with lime in Brazilian soils, and pH is increased to approximately 6.0. At that level of pH, most of the soil samples in the present study adsorbed between 70% and 100% of the total Se(IV) in solution in our experiments.

The Se(IV) adsorption data fell into 2 distinct groups of soils. The first comprises soils in which a gradual decrease of Se(IV) adsorption was observed as pH increased (Figures 1–3). A different trend was observed in the second group (LAwf, LVef, LVwf-A, LVwf-B, MT, and NVef; Figures 1 and 2). In these soils, a plateau was observed at low pH values. Decreases in Se(IV) adsorption were observed under more alkaline conditions, starting at pH values of approximately 7 (Figure 2).

The only soil with high organic carbon content (GM) had a special trend, because adsorption was less affected by pH increases than for the other soils across the entire pH range (Figure 1). In a laboratory study, Se(IV) was strongly adsorbed by pure humic acid in solution [33]. The sandy-textured soils (LVA-2, PVA-3, RL, and RQ; Figure 3) had lower Se(IV) adsorption. The main soil compounds responsible for Se(IV) adsorption are present in the clay fraction [34]. In Indian soils, a significant correlation was observed between Se(IV) adsorption and clay content [12]. The soil samples CX, LA-1, LV-2, and PV-2 (Figure 1) had a high clay content, although a constant decrease in Se(IV) adsorption with increasing pH was observed. This may reflect the fact that the mineralogy of these soils is primarily kaolinite, as described by Bar-Yosef and Meek [35]. Both LVA-2 and PVA-3 (Figure 3) have similar textures, but showed different Se(IV) adsorption trends because of the higher concentration of Fe oxides in PVA-3.

The highest levels of Se(IV) adsorption, even at high pH, occurred in soils with the highest degree of weathering: LAwf, LVef, LVwf-A, LVwf-B, MT, and NVef (Figures 1 and 2). These soils had high amounts of oxides and exhibited maximum Se(IV) adsorption across a large range of pH, decreasing only at medium alkalinity. The high affinity of Se(IV) for these minerals is well known, as it is for hematite [11,36], goethite [37], aluminum oxide [38], and magnetite [39]. Two soils, LVwf-A and LVwf-B (Figure 2), are superficial and subsurface samples

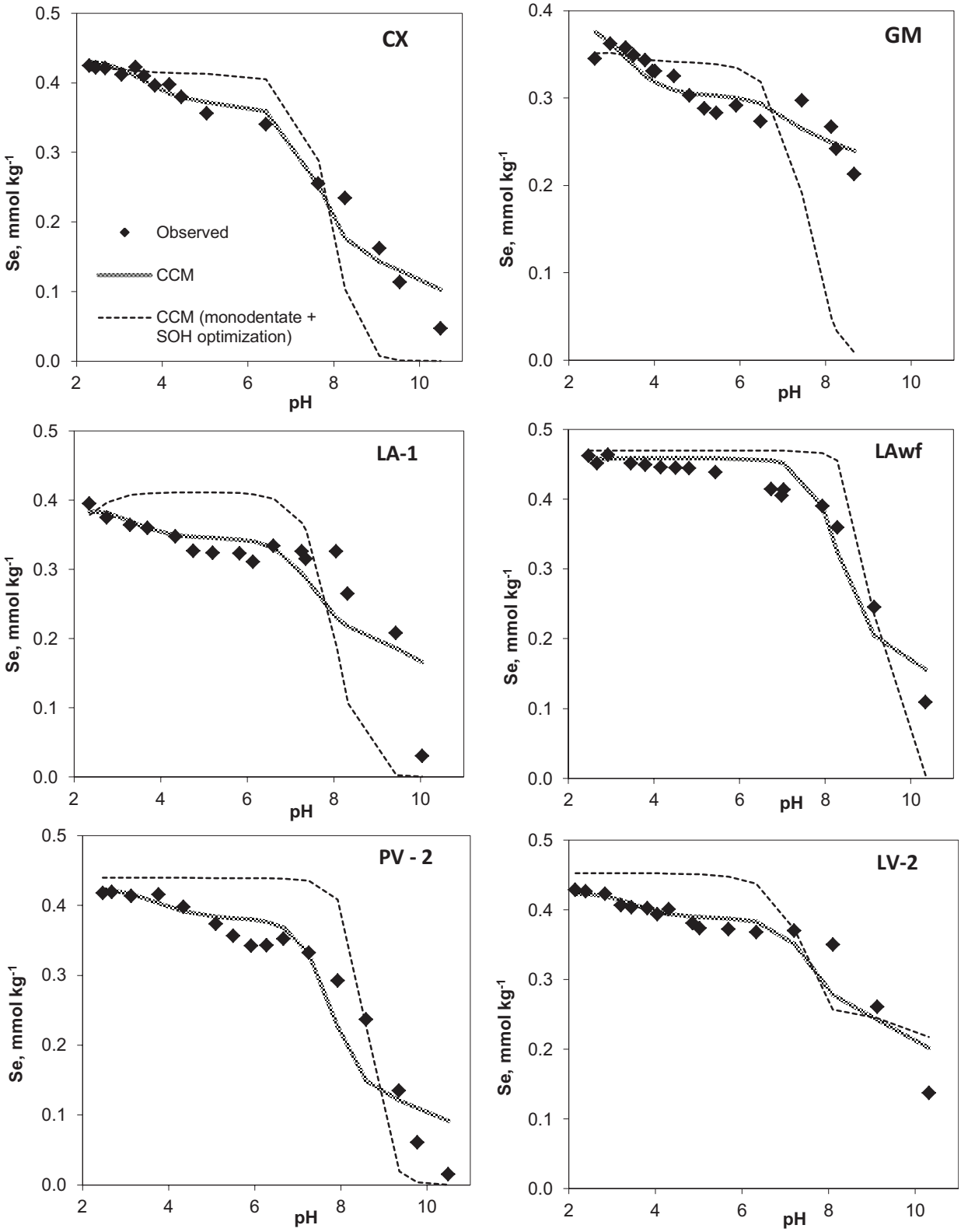

Figure 1. Se(IV) adsorption envelopes of the soils with the highest adsorption, showing the fit of the constant capacitance model (CCM). See Table 1 for descriptions of soil samples.

of the same soil profile horizons, respectively. In the B-horizon, adsorption of Se(IV) was higher than in the superficial horizon at pH higher than 6.7, probably because of the lower amount of organic carbon covering the surfaces of the oxide colloids.

Effect of pH on Se(VI) adsorption

The Se(VI) adsorption was lower than Se(IV) adsorption on the soils, as has been reported previously by several authors [7,13,14]. This is a consequence of the weak bonding of

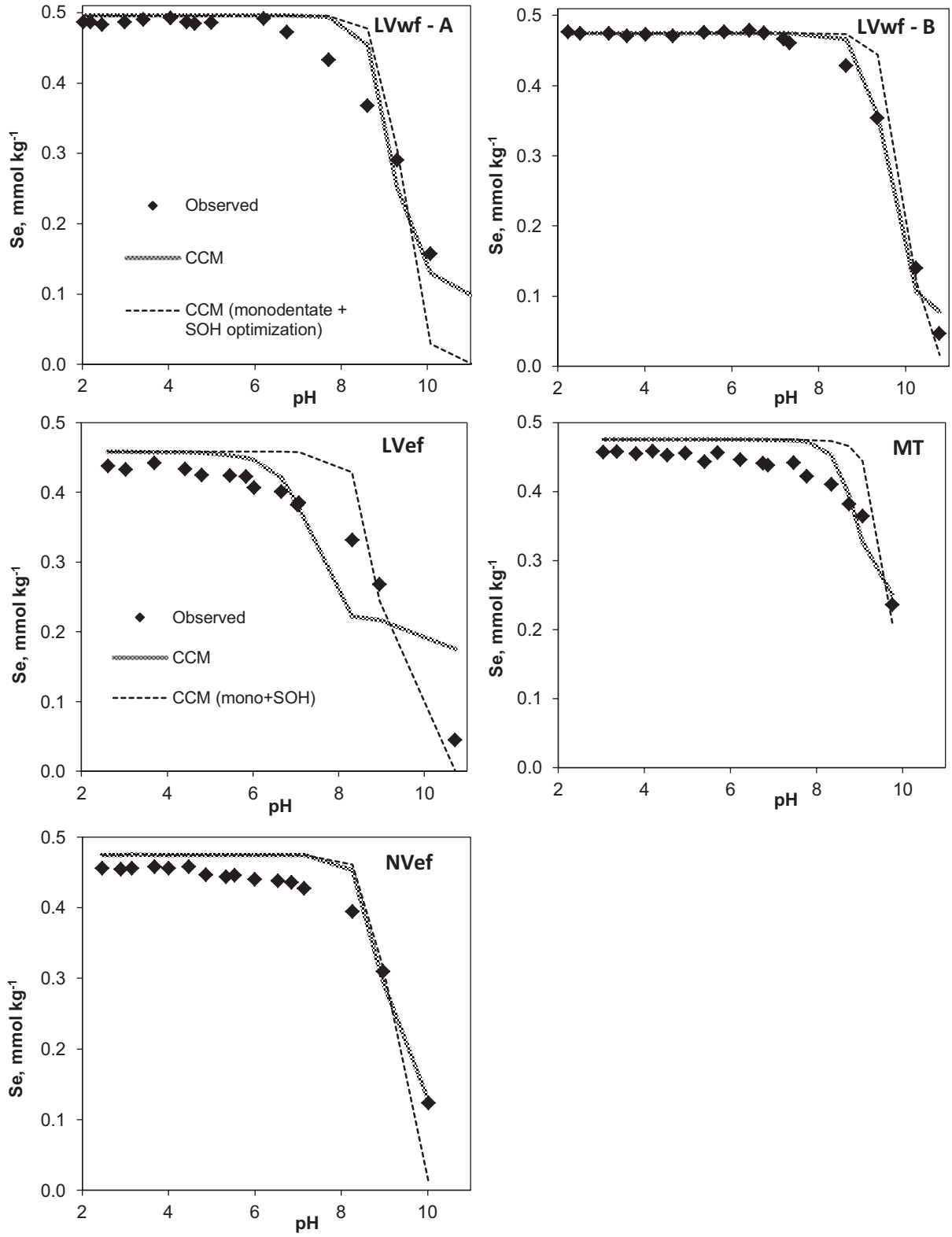

Figure 2. Se(IV) adsorption envelopes of the soils with the median-high adsorption, showing the fit of the constant capacitance model (CCM). See Table 1 for descriptions of soil samples.

Se(VI) with iron oxide [6]. The Se(VI) adsorption behavior was similar for most soil samples, and maximum Se(VI) adsorption was observed at the lowest pH. Adsorption decreased sharply with increasing solution pH until around pH 4, and it was very low at higher pH values (Figures 4–6). In this case, Se(VI) adsorption becomes negligible for pH values between 5.5 and 6.5, commonly found in Brazilian agricultural soils. Organic matter was not an important soil component for Se(VI), diverging from the observed for Se(IV) adsorption as can be seen in soil GM (Figure 6). This behavior was explained by Loffredo et al. [40] as a consequence of the low zero point of charge of the humic substances.

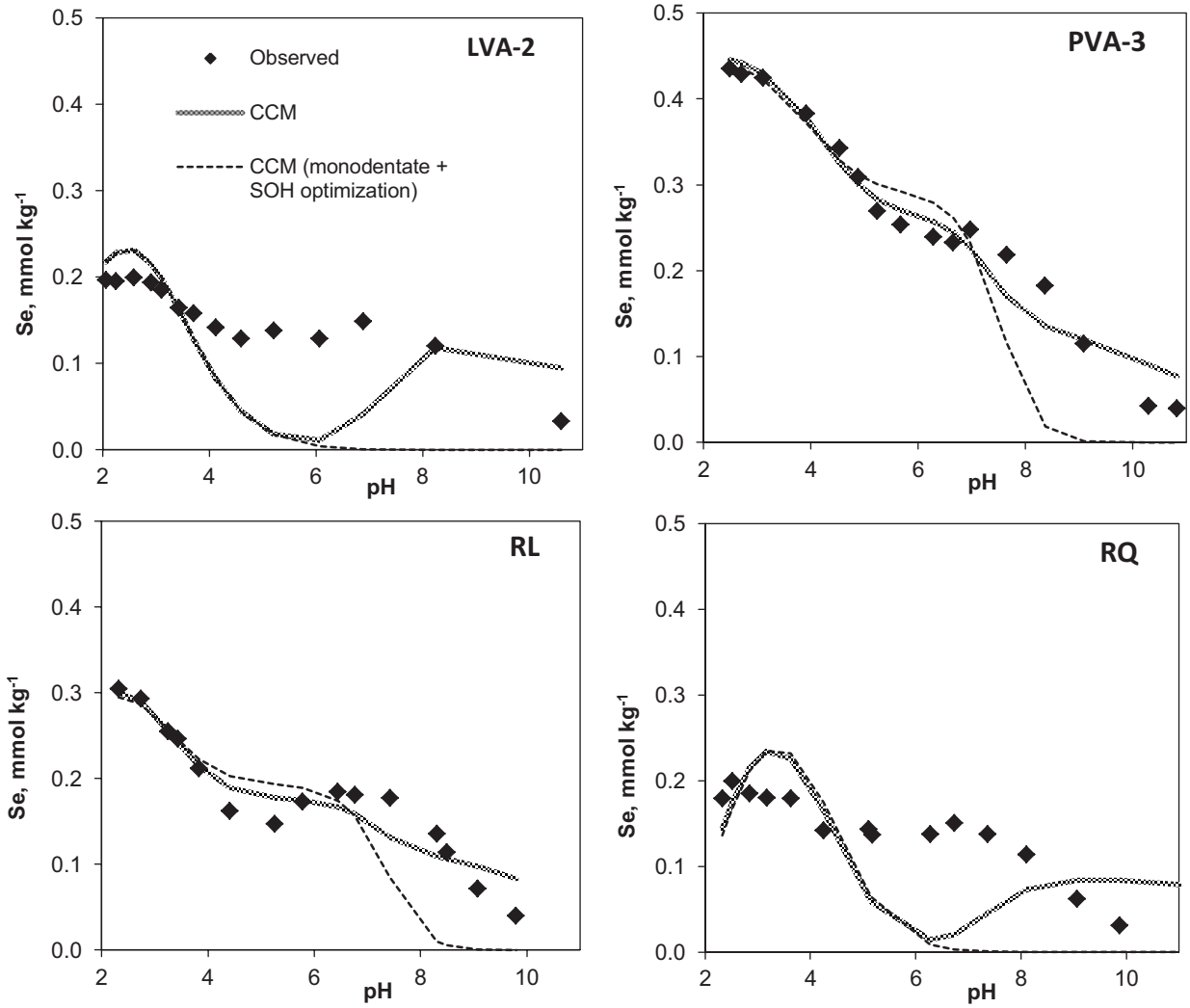

Figure 3. Se(IV) adsorption envelopes of the soils with the lowest adsorption, showing the fit of the constant capacitance model (CCM). See Table 1 for descriptions of soil samples.

As observed in the adsorption of Se(IV), Se(VI) adsorption was very low in soils with a high sand content (LVA-2, PVA-3, RL, and RQ in Figures 5 and 6). This negative correlation between Se(VI) adsorption in sandy- to sandy–loamy-textured soils has been reported for tropical soils [41]. Low amounts of adsorbed Se(VI) were observed in 18 sandy-textured soils from the United States (clay contents between 10 g kg^{-1} and 29 g kg^{-1}), and decreased gradually as pH increased in soil containing 5.22 μmol L^{-1} of Se [13].

The only exception to this trend among the soils was the Rhodic Acrudox at both depths (LVwf-A and LVwf-B in Figure 4). Soils LVwf showed a maximum Se(VI) adsorption higher than those of all other soils: 100% in LVwf compared with less than 70% in the others. The second difference observed in the LVwf soils was a plateau of maximum adsorption up to pH values of 3.5 and 4.5 (A- and B-horizons, respectively, of LVwf). At higher pH levels, Se(VI) adsorption decreased with increasing soil solution pH, and became very low at pH values higher than 6.5 and 7.5, for superficial and subsurface samples, respectively. A possible cause of such behavior is the high amount of oxides present in the LVwf samples (208 g kg^{-1} and 232 g kg^{-1} of DCB-Fe for the A- and B-horizons, respectively).

Adsorption of Se(VI) on pure oxides has been studied in detail. Rovira et al. [11] described Se(VI) adsorption on hematite and goethite, both of which adsorbed high amounts of Se(IV) but with different curve trends. The Se(VI) adsorption on goethite decreased gradually with increasing pH. In contrast, Se(VI) adsorption on hematite was similar to Se(VI) adsorption in LVwf soils; the maximum adsorption was observed at pH 6. This difference in affinity was explained by Peak and Sparks [9] as follows: Se(VI) only forms inner-sphere surface complexes on hematite, but it forms a mixture of outer- and inner-sphere surface complexes on goethite. Peak [38] evaluated Se(VI) adsorption on a pure Al oxide and found a curve similar to that observed for the LVwf samples. These results reinforce the importance of hematite and aluminum oxides in Se(VI) adsorption on highly weathered tropical soils.

Chemical modeling of Se adsorption on soil

For both Se(IV) and Se(VI), the surface complexation constants were optimized separately for monodentate and bidentate inner-sphere surface complexation constants. In Se(IV) optimization, only the species $SHSeO_3$ ($\log {}^1K_{Se(IV)}$) did not converge. The simultaneous optimization of monodentate ($SSeO_3^-$) and bidentate (S_2SeO_3) improved the quality of fit, when evaluated by goodness-of-fit, V_Y, an error parameter calculated by the FITEQL software. In addition, protonation constant values were optimized simultaneously with the former

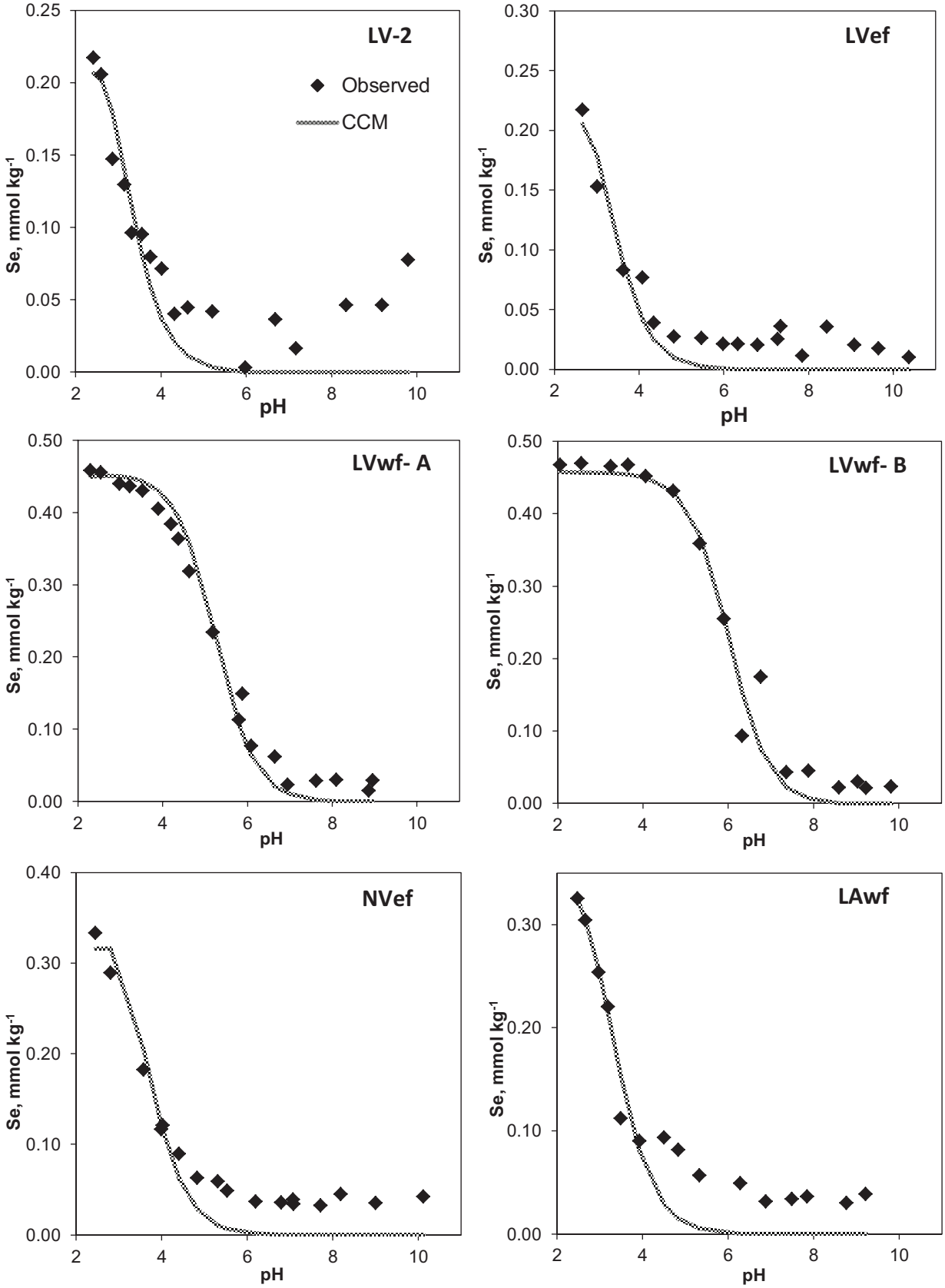

Figure 4. Se(VI) adsorption envelopes of the soils with the highest adsorption, showing the fit of the constant capacitance model (CCM). See Table 1 for descriptions of soil samples.

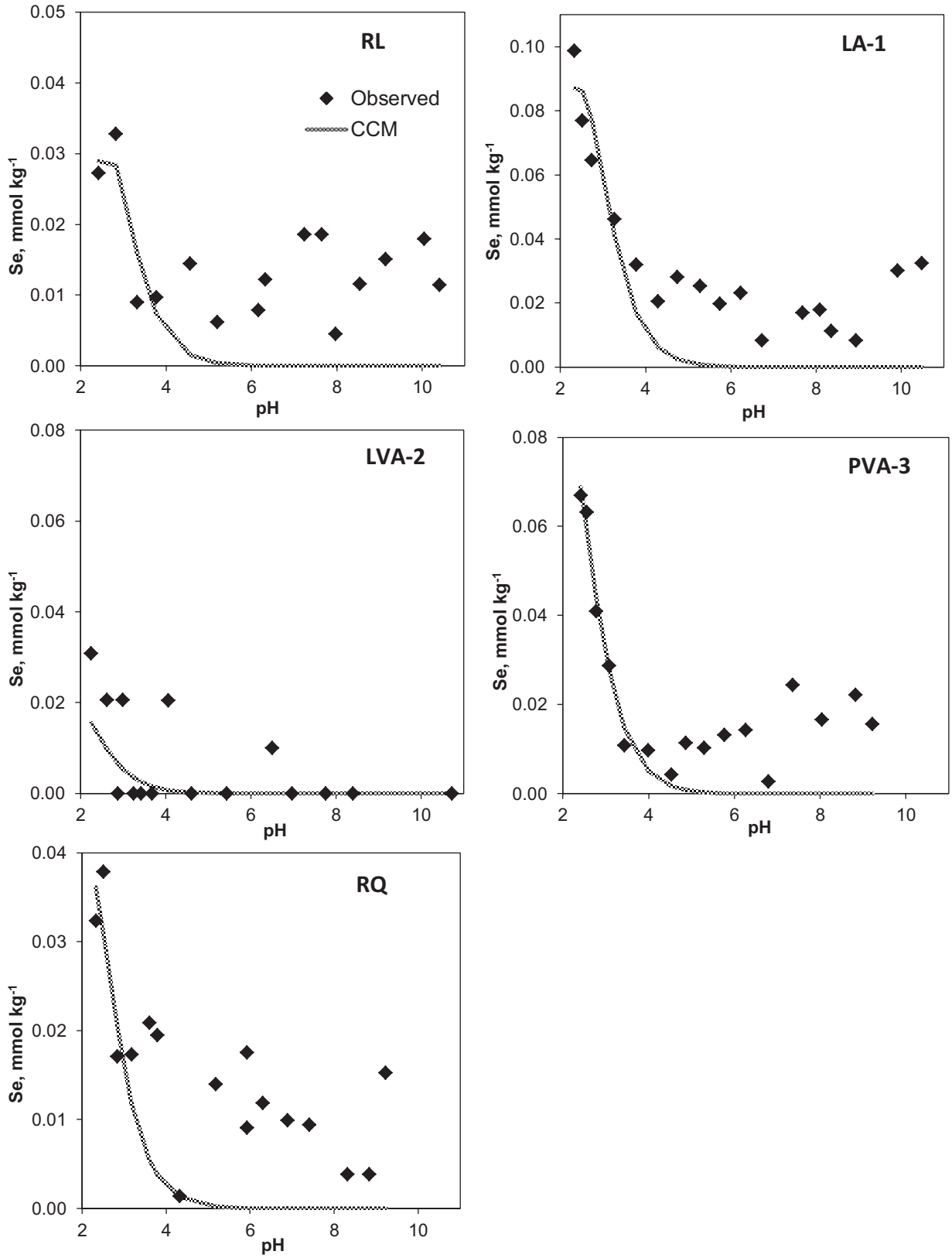

Figure 5. Se(VI) adsorption envelopes of the soils with the lowest adsorption, showing the fit of the constant capacitance model (CCM). See Table 1 for descriptions of soil samples.

optimization (log $K^2_{Se(IV)}$ and log $K^3_{Se(IV)}$) to improve model fit. These optimizations did not converge for 5 soil samples with higher oxide content (LVef, LVwf-A, LVwf-B, MT, and NVef). The complexation constants were underpredicted for the 2 sandy-textured soils (LVA-2 and RQ) that adsorbed low amounts of Se(IV). All surface complexation constants from each soil sample and their respective errors are provided in Table 2. In a study of selenite adsorption envelopes carried out

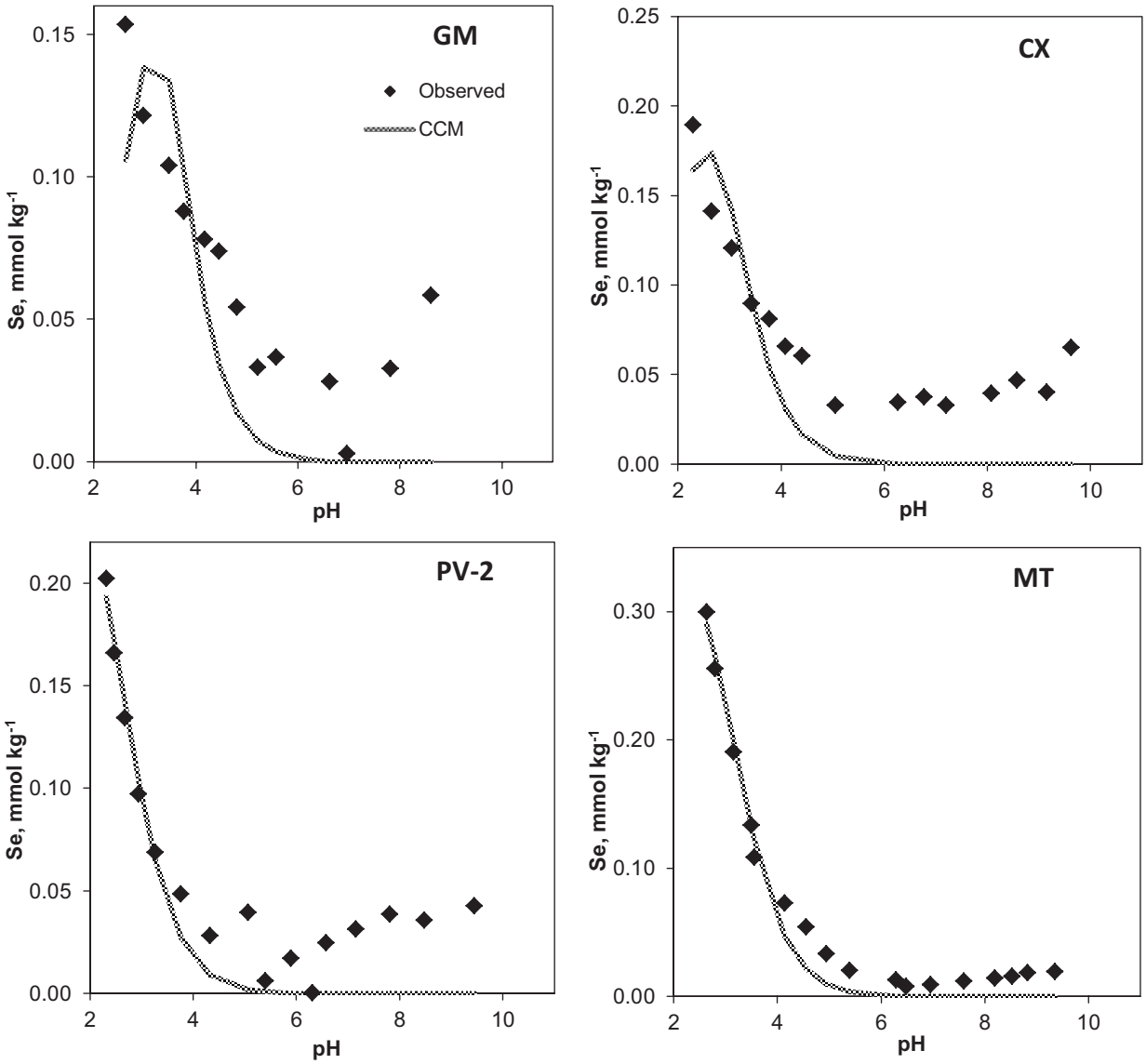

Figure 6. Se(VI) adsorption envelopes of the soils with median adsorption, showing the fit of the constant capacitance model (CCM). See Table 1 for descriptions of soil samples.

Table 2. Constant capacitance model surface complexation constants and goodness of fit (error) in the pH-dependent adsorption of Se IV

Soil[a]	log $K^2_{Se(IV)}$	log $K^3_{Se(IV)}$	log K_+ (int)	Variance[b]
CX	0.371	–5.532	2.542	0.882
GM	–0.518	–6.140	2.161	0.487
LA-1	0.473	–4.936	2.070	3.791
LAwf	1.054	–6.030	1.251	1.127
LV-2	0.369	–5.490	2.325	1.111
LVA-2	–3.295	–3.527	8.494	7.205
LVef	–0.440	–5.792	NC	4.349
LVwf-A	2.208	–6.207	NC	1.497
LVwf-B	3.169	–5.924	NC	0.371
MT	1.761	–6.239	NC	1.099
NVef	1.929	–6.165	NC	1.231
PV-2	0.373	–6.013	2.703	2.575
PVA-3	0.054	–5.288	3.448	1.123
RL	–0.409	–5.659	2.491	0.949
RQ	–2.606	–1.957	9.578	8.254

[a]See Table 1 for descriptions of soil samples.
[b]Goodness of fit equals the sum of squares divided by the degrees of freedom.
NC = no convergence.

with 45 soil samples from the United States, Goldberg et al. [27] obtained optimization only for log $K^2_{Se(IV)}$ and log K_+ (int). On average, the surface complexation constants for the US soils were lower than the constants observed for tropical Brazilian soil samples.

Inner-sphere surface complexation is an assumption of the CCM. Selenate complexation on soil components is not totally understood, however. Some researchers have reported weak bonding of Se(VI) to soil surface complexes [6,9,11]. In the present study, inner-sphere surface complexation was taken into account in the Se(VI) adsorption data, as it has been already described for clay minerals [8,38,42].

The 2 monodentate surface complexation constants for species ($SHSeO_4$ and $SSeO_4^-$) were optimized simultaneously and produced a lower data fit error (Table 3). The optimizations of Se(VI) bidentate complexation ($\log K^3_{Se(VI)}$) and the protonation complex ($\log K_+$ (int)) did not converge for any of the Se(VI) adsorption data. Three soil samples (LVA-2, LVwf-B, and PV-2) did not converge for log $K^2_{Se(VI)}$, as a consequence of the very low concentration of $SSeO_4^-$ ($<10^{-35}$) complexed in the soil surface. The distinctive Se(VI) adsorption

Table 3. Constant capacitance model surface complexation constants and goodness of fit (error) values in the pH-dependent adsorption of Se VI

Soil[a]	log $K^1_{se(VI)}$	log $K^2_{se(VI)}$	Variance[b]
CX	3.605	–0.853	2.355
GM	3.552	–0.265	1.441
LA-1	3.247	–0.939	0.609
LAwf	3.587	–2.044	2.487
LV-2	3.435	–1.273	1.847
LVA-2	2.723	NC	1.293
LVef	3.396	–1.167	0.888
LVwf-A	5.407	–1.023	0.992
LVwf-B	6.347	NC	1.778
MT	3.226	–2.509	0.466
NVef	3.856	–1.129	1.906
PV-2	3.043	NC	0.925
PVA-3	2.895	–2.463	0.255
RL	2.738	–0.755	0.228
RQ	3.715	–0.739	0.185

[a]See Table 1 for descriptions of soil samples.
[b]Goodness of fit equals the sum of squares divided by the degrees of freedom. NC = low concentration of $SSeO^{4-}$ ($<10^{-35}$).

on LVwf described previously is reflected by the higher log $K^1_{Se(VI)}$ constant compared with the other soil samples. Considering the lower average of the goodness of fit parameter, it is possible to suggest that inner-sphere surface complexation is predominant in highly weathered Brazilian tropical soils. As a consequence, Se(VI) is strongly adsorbed, which may influence the rate of fertilizer applied to highly weathered soils, because Brazilian tropical soils have low amounts of Se [43].

One of the advantages of using the CCM is the ability to calculate the distribution of Se surface species on soils as a function of varying pH [16]. The effect of variation in pH on the distributions of the Se(IV) and Se(VI) species adsorbed to each soil surface was calculated, and some examples are shown in Figure 7. The selenite species adsorbed in tropical soils were $SSeO_3^-$ and S_2SeO_3, with predominance of the monodentate complex. The proportion of S_2SeO_3 was greater than that of $SSeO_3^-$ only under alkaline conditions (high pH values), varying between 6 and 10. The pH value at which the conversion from 1 species to another occurred increased with increasing oxide content.

The 2 species of Se(VI) were the monodentate complexes, $SHSeO_4$ and $SSeO_4^-$. The predominant species was $SHSeO_4$ for

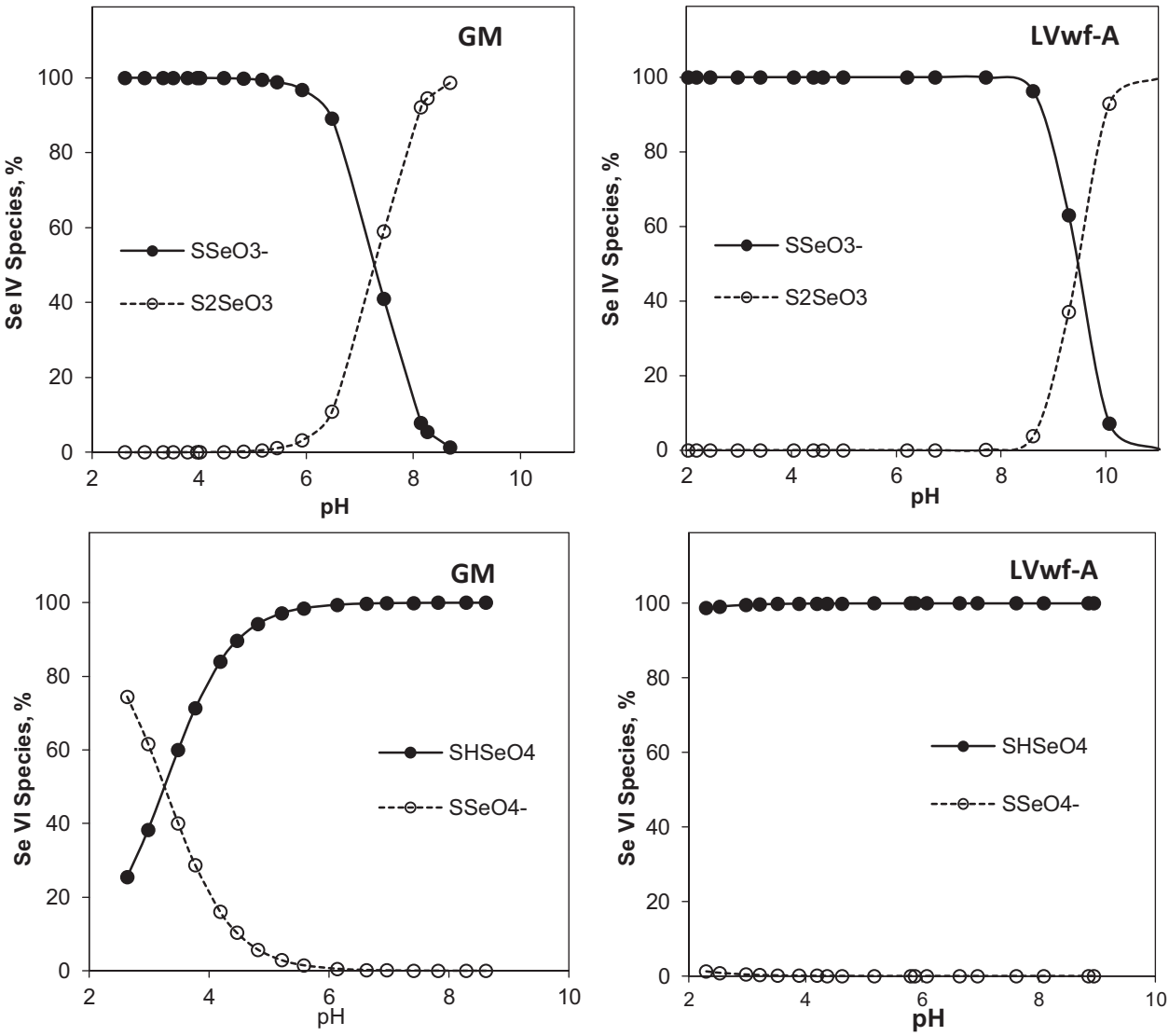

Figure 7. Examples of calculated Se(IV) and Se(VI) surface species on soils with varying pH. See Table 1 for descriptions of soil samples.

all of the soil samples. It was the only species for the soil samples in which Se(VI) adsorption was high. The $\equiv SSeO_4$ species was predominant at low pH values (<4) in some soil samples (CX, GM, LA-1, and RL). The probable species under natural pH values found in soils would be $\equiv SHSeO_4$. The surface complexation constants obtained in our model application are conditional because protonation constant values were either fixed for all soils for Se(VI) adsorption or optimized with the Se(IV) adsorption constants. Nevertheless, the approach is superior to the completely empirical Langmuir and Freundlich adsorption isotherm approach because our model considers surface charge and pH dependence of selenium adsorption.

In conclusion, at the pH range commonly found in the majority of the soils (4.5–7.0), Se(IV) is strongly adsorbed on the surface of soil colloids, which makes it difficult for the plants to take up. In contrast, Se(VI) adsorption is low on soils at the same pH range. However, Se adsorption is high even for the Se(VI) species in highly weathered soils with positive balance of charge.

Acknowledgment—We thank the Brazilian funding agencies CAPES and CNPQ for M.B. Gabos's scholarships in Brazil and the United States, respectively. We also thank the US Department of Agriculture Agricultural Research Service, US Salinity Laboratory, for support with the experimental analysis.

REFERENCES

1. Kabata-Pendias A, Mukherjee AB. 2007. *Trace Elements from Soil to Human*. Springer-Verlag, New York, NY, USA.
2. Minorsy PV. 2003. Selenium in plants. *Plant Physiol* 133:14–15.
3. Kabata-Pendias A. 2010. *Trace Elements in Soil and Plants*, 3rd ed. CRC Press, Boca Raton, FL, USA.
4. Tan J, Zhu W, Wang W, Li R, Hou S, Wang D, Yang L. 2002. Selenium in soil and endemic diseases in China. *Sci Total Environ* 284:227–235.
5. Keskinen R, Päivi E, Yli-Halla M, Hartikainen H. 2009. Efficiency of different methods in extracting selenium from agricultural soils of Finland. *Geoderma* 153:87–93.
6. Hayes KF, Roe AL, Brown GE, Hodgson KO, Leckie JO, Parks GA. 1987. In situ X-ray absorption study of surface complexes: Selenium oxyanions on α-FeOOH. *Science* 238:783–786.
7. Goh KH, Lim TT. 2004. Geochemistry of inorganic arsenic and selenium in a tropical soil: Effect of reaction time, pH and competitive anions on arsenic and selenium adsorption. *Chemosphere* 55:849–859.
8. Manceau A, Charlet L. 1994. The mechanism of selenate adsorption on goethite and hydrous oxide. *J Colloid Interface Sci* 168:87–93.
9. Peak D, Sparks DL. 2002. Mechanisms of selenate adsorption on iron oxides and hydroxides. *Environ Sci Technol* 36:1460–1466.
10. Foster AL, Brown GE, Parks GA. 2003. X-ray absorption fine structure study of As(V) and Se(IV) sorption complexes on hydrous Mn oxides. *Geochim Cosmochim Acta* 67:1937–1953.
11. Rovira M, Giménez J, Martínez M, Martínez-Lladó X, Pablo J, Martí V, Duro L. 2008. Sorption of selenium(IV) and selenium(VI) onto natural iron oxides: Goethite and hematite. *J Hazard Mater* 150:279–284.
12. Dhillon KS, Dhillon SK. 1999. Adsorption–desorption reactions of selenium in some soils of India. *Geoderma* 93:19–31.
13. Hyun S, Burns PE, Murarka I, Lee LS. 2006. Selenium(IV) and (VI) Sorption by soils surrounding fly ash management facilities. *Vadose Zone J* 5:1110–1118.
14. Barrow NJ, Whelan BR. 1980. Testing a mechanistic model, VII. The effects of pH and of electrolyte on the reaction of selenite and selenate with a soil. *J Soil Sci* 40:17–28.
15. Sposito G. 1983. Foundations of surface complexation models of the oxide–Aqueous solution interface. *J Colloid Interface Sci* 91:329–340.
16. Goldberg S, Lesch SM, Suarez DL. 2007. Predicting selenite adsorption by soils using soil chemical parameters in the constant capacitance model. *Geochim Cosmochim Acta* 71:5750–5762.
17. Goldberg S, Glaubig RA. 1988. Anion sorption on a calcareous, montmorillonitic soil—Selenium. *Soil Sci Soc Am J* 52:954–958.
18. Goldberg S, Hyun S, Lee LS. 2008. Chemical modeling of arsenic (III, V) and selenium (IV, VI) adsorption by soils surrounding ash disposal facilities. *Vadose Zone J* 7:1231–1238.
19. Cihacek LJ, Bremner JM. 1979. A simplified ethylene glycol monoethyl ether procedure for assessing soil surface area. *Soil Sci Soc Am J* 43: 821–822.
20. Coffin DE. 1963. A method for the determination of free iron oxide in soils and clays. *Can J Soil Sci* 43:7–17.
21. Gillman GP. 1979. A proposed method for the measurement of exchange properties of highly weathered soils. *Aust J Soil Res* 17:129–139.
22. Soares MR. 2004. Distribution coefficient (*K*d) of heavy metals in soil of the State of São Paulo. PhD thesis (in Portuguese). University of São Paulo, São Paulo, Brazil.
23. Stumm W, Kummert R, Sigg L. 1980. A ligand exchange model for the adsorption of inorganic and organic ligands at hydrous oxide interfaces. *Croat Chem Acta* 53:291–312.
24. Goldberg S. 1992. Use of surface complexation models in soil chemical systems. *Adv Agron* 47:233–329.
25. Karamalidis KA, Dzombak DA. 2010. *Surface Complexation Modeling: Gibbsite*. John Wiley & Sons, Hoboken, NJ, USA.
26. Herbelin AL, Westall JC. 1999. FITEQL: A computer program for determination of chemical equilibrium constants from experimental data. Rep. 99-01, Version 4.0. Department of Chemistry, Oregon State University, Corvallis, OR, USA.
27. Goldberg S, Criscenti LJ, Turner DR, Davis JA, Cantrell KJ. 2007. Adsorption-desorption processes in subsurface reactive transport modeling. *Vadose Zone J* 6:407–435.
28. Westall J, Hohl H. 1980. A comparison of electrostatic models for the oxide/solution interface. *Adv Colloid Interface Sci* 12:265–294.
29. Goldberg S, Sposito G. 1984. A chemical model of phosphate adsorption by soils. I. Reference oxide minerals. *Soil Sci Soc Am J* 48:772–778.
30. Davis JA, Kent DB. 1990. Surface complexation modeling in aqueous geochemistry. *Rev Mineral* 23:177–260.
31. Alleoni LRF, Peixoto RTG, Azevedo AC, Melo LCA. 2009. Components of surface charge in tropical soils with contrasting mineralogies. *Soil Sci* 174:629–638.
32. Lee S, Doolittle JJ, Woodard HJ. 2011. Selenite adsorption and desorption in selected South Dakota soils as a function of pH and other oxyanions. *Soil Sci* 176:73–79.
33. Kamei-Ishikawa N, Nakamaru Y, Tagami K, Uchida S. 2008. Sorption behavior of selenium on humic acid under increasing selenium concentration solid/liquid ratio. *J Environ Radioactiv* 99:993–1002.
34. Goldberg S. 2011. Chemical equilibrium and reaction modeling of arsenic and selenium in soils. In Selim M, ed, *Dynamics and Bioavailability of Heavy Metals in the Rootzone*. CRC Press, Boca Raton, FL, USA, p 65–92.
35. Bar-Yosef B, Meek D. 1987. Selenium sorption by kaolinite and montmorillonite. *Soil Sci* 144:11–19.
36. Duc M, Lefevre G, Fedoroff M. 2006. Sorption of selenite ions on hematite. *J Colloid Interface Sci* 298:556–563.
37. Hiemstra T, Riemsdijk WH. 1999. Surface structural ion adsorption modeling of competitive binding of oxyanions by metal (hydr)oxides. *J Colloid Interface Sci* 210:182–193.
38. Peak D. 2006. Adsorption mechanisms of selenium oxyanions at the aluminum oxide/water interface. *J Colloid Interface Sci* 303:337–345.
39. Martínez M, Giménez J, Pablo J, Rovira M, Duro L. 2006. Sorption of selenium(IV) and selenium(VI) onto magnetite. *Appl Surf Sci* 252:3767–3773.
40. Loffredo N, Mounier Y, Thiry Y, Coppin F. 2011. Sorption of selenate on soil and pure phases: Kinetic parameters and stabilization. *J Environ Radioactiv* 102:843–851.
41. Abreu LB, Carvalho GS, Curi N, Guilherme LRG, Marques JJ. 2011. Selenium sorption in soils of the cerrado biome. *Braz J Soil Sci* (in Portuguese) 35:1995–2003.
42. Su C, Suarez DL. 2000. Selenate and selenite sorption on iron oxides: An infrared and electrophoretic study. *Soil Sci Soc Am J* 64:101–111.
43. Gabos MB. 2012. Background concentrations and adsorption of selenium in tropical soils. PhD thesis. University of São Paulo, São Paulo, Brazil. [cited 2013 February 17]. Available from: http://www.teses.usp.br/teses/disponiveis/11/11140/tde-20092012-1647 03/pt-br.php.